SECRET

RM SA53C18

NACA RM SA53C18

NACA

RESEARCH MEMORANDUM

for the

U. S. Air Force

WIND-TUNNEL INVESTIGATION OF A 1/60-SCALE MODEL OF THE REPUBLIC MX-1554 AIRPLANE AT A MACH NUMBER OF 2.85

By Robert R. Dickey and J. Richard Spahr

Ames Aeronautical Laboratory
Moffett Field, Calif

NATIONAL ADVISORY COMMITTEE FOR AERONAUTICS

WASHINGTON

Mar. 18, 1953

14

SECRET

NATIONAL ADVISORY COMMITTEE FOR AERONAUTICS

RESEARCH MEMORANDUM

for the

U. S. Air Force

WIND-TUNNEL INVESTIGATION OF A 1/60-SCALE MODEL OF THE REPUBLIC MX-1554 AIRPLANE AT A MACH NUMBER OF 2.85

By Robert R. Dickey and J. Richard Spahr

SUMMARY

A wind-tunnel investigation was performed to determine the static longitudinal and lateral stability and the control characteristics of a 1/60-scale model of the Republic MX-1554 airplane at a Mach number of 2.85 and a Reynolds number of 2.45 million based on the mean aerodynamic chord of the wing. The results of the investigation are presented without analysis or discussion to expedite publication of the data.

INTRODUCTION

The Republic MX-1554 airplane was designed for the purpose of combating high-performance enemy bombers flying at Mach numbers up to 1.3. At the request of the U. S. Air Force, a wind-tunnel investigation has been made at a Mach number of 2.85 to determine the static longitudinal and lateral stability and the control characteristics of a 1/60-scale model of the airplane. The results of a similar investigation of a 1/15-scale model at Mach numbers of 1.45 and 1.90 are presented in reference 1, and an extensive investigation of the low-speed stability and control characteristics of a 1/10-scale model of the airplane is reported in reference 2.

NOTATION

The axis system shown in figure 1 was used in reducing the data to standard NACA coefficient form. The moment reference point was at 35 percent of the wing mean aerodynamic chord and on a line parallel to the wing-chord plane through the center of the duct exit.

The coefficients and symbols used are defined as follows:

A_e area of duct at the exit, sq in.

b total wing span, in.

C_D drag coefficient, $\frac{\text{fore drag} - D_i}{qS}$

C_L lift coefficient, $\frac{\text{lift}}{qS}$

C_l rolling-moment coefficient, $\frac{\text{rolling moment}}{qSb}$

C_m pitching-moment coefficient, $\frac{\text{pitching moment}}{qS\bar{c}}$

C_n yawing-moment coefficient, $\frac{\text{yawing moment}}{qSb}$

C_Y side-force coefficient, $\frac{\text{side force}}{qS}$

$\bar{c}$ mean aerodynamic wing chord, in.

D_b base drag, lb

D_i internal duct drag, lb

i_H incidence angle of horizontal tail (positive when trailing edge down), deg

i_W incidence angle of wing (positive when trailing edge down), deg

M_o free-stream Mach number

M_e Mach number of internal flow at duct exit

m mass flow through duct, slugs/sec

P_b base pressure, lb/sq in.

p_e static pressure at duct exit, lb/sq in.

p_o free-stream static pressure, lb/sq in.

p_t free-stream total pressure, lb/sq in.

q free-stream dynamic pressure, lb/sq in.

S total wing area formed by extending the leading and trailing edges to the center line of the body, sq in.

S_b area of solid portion of model base, sq in.

V_e velocity of internal flow at duct exit, ft/sec

V_o free-stream velocity, ft/sec

α angle of attack, deg

β angle of sideslip, deg

δ_a aileron deflection (positive deflection downward), deg

δ_e elevator deflection (positive deflection downward), deg

δ_r rudder deflection (positive deflection to the left), deg

Configuration Designations (See fig. 2.)

B body

W wing

H horizontal tail

V_L large vertical tail

V_S small vertical tail

APPARATUS

The tests were conducted in the Ames 1- by 3-foot supersonic wind tunnel No. 2. This wind tunnel is an intermittent-operation, non-return tunnel in which both Mach number and Reynolds number are variable.

A three-view drawing of the 1/60-scale ducted model of the Republic MX-1554 airplane used in this investigation is shown in figure 2, and some of the pertinent dimensions of the model are listed in table I. The forward part of the fuselage was a pointed body of revolution which faired into a flat-sided section aft of the scoop inlet which was mounted on the underside of the fuselage. Although the inlet area for the full-scale airplane is variable in flight, the model used for this investigation had a fixed inlet area designed for a Mach number of 3.1. A solid wedge-shaped divider

was mounted in front of the scoop for the purpose of diverting the boundary-layer air from the inlet. The wing had swept-back leading and trailing edges with zero taper ratio and modified NACA 65A003 airfoil sections. The horizontal tail was mounted low on the fuselage well below the extended wing-chord plane. The incidence angle of both the wing and the horizontal tail could be varied. The model had interchangeable vertical tails of the same plan form but of two different areas. Only the larger vertical tails were provided with deflected rudder controls. All control surfaces were of the unshielded horn-balanced type with the deflected controls machined as integral parts of the main wing or tail surfaces. A series of interchangeable wings and tails with various angles of control deflection provided for a range of control settings. For lateral control, only one aileron was deflected on each wing. The model was supported from the rear by a sting-type support which fitted into the base of the model and divided the duct into two parts.

The forces and moments on the model were measured by means of a four-component strain-gage balance. The model was instrumented for the measurement of static pressures at two points along the duct and at the base of the model.

TESTS AND PROCEDURE

All tests were conducted at a Mach number of 2.85 and a Reynolds number of 2.45 million based on the mean aerodynamic chord of the wing. For the angle-of-attack tests, the model was mounted in the tunnel with the wing horizontal and then was pitched through a nominal angle-of-attack range from -5° to $+5^\circ$, while the lift, drag, pitching moment, and rolling moment were measured. For the sideslip tests, the model was mounted with the wing vertical and was yawed through a range of sideslip angles from -5° to $+5^\circ$, while the side force, drag, yawing moment, and rolling moment of the model were measured. During all these tests, the base pressure and internal-duct pressures were measured.

All the drag results presented represent the external fore drag and were obtained by subtracting the base drag and the internal drag through the duct from the total measured drag. The base drag was calculated from the measured pressures by means of the relation

$$D_b \equiv (p_o - p_b) S_b$$

The internal drag of the air flow through the engine duct was assumed to be given by the expression

$$D_i = m (V_o - V_e) + A_e (p_o - p_e)$$

which is based upon the assumption that the Mach number and total pressure of the air approaching the duct inlet are the same as those existing in the free stream. It is estimated, however, that the drag error caused by this assumption is within the accuracy of the drag measurements. The static pressures measured in the duct indicated that the flow was choked at the exit ($M_e = 1$) throughout the investigation, and hence the foregoing expression for internal drag was simplified to

$$D_i = 0.0582\, p_e + 0.0068\, p_t$$

Schlieren photographs showing the flow at the duct inlet for several angles of attack are shown in figure 3. These photographs indicate that no detached shock waves are present at the inlet.

The nominal values of α and β were corrected for deflections of the balance and support caused by aerodynamic loads. These deflections were measured from enlargements of schlieren photographs of the model obtained during the tests.

The lift and pitching-moment data have been corrected for tunnel stream-angle effects. No stream-angle correction has been applied to the rolling moment for the model in pitch or to any of the sideslip data; however, since the airplane is symmetrical in sideslip, a combined correction for stream angle and model asymmetry may be made by shifting the data through the origin.

The precision of the experimental data has been estimated, and the following average values were obtained for the uncertainty in the measured quantities:

C_L and C_Y	± 0.0010
C_m	$\pm .0020$
C_n	$\pm .0008$
C_l	$\pm .0002$
C_D	$\pm .0010$
α and β	$\pm .08^\circ$
δ_a, δ_e, δ_r, i_H, and i_W	$\pm .10^\circ$

RESULTS

The aerodynamic characteristics in pitch for both the model build-up and the control-effectiveness tests are presented in figure 4, and the corresponding aerodynamic characteristics in sideslip are presented in figure 5. A summary of some of the aerodynamic parameters obtained from both the lateral and longitudinal tests is given in table II.

The increment of rolling-moment coefficient that is present at zero angle of attack for all winged configurations in pitch (fig. 4) is apparently caused primarily by wing asymmetry rather than stream nonuniformities, since a rolling moment of the same magnitude is also present at zero sideslip angle in the sideslip tests (fig. 5) for which the wing was in a vertical plane. The rolling-moment data for some of the angles of sideslip are not presented in figure 5 because of the malfunctioning of the rolling-moment instrumentation during these tests.

Ames Aeronautical Laboratory
National Advisory Committee for Aeronautics
Moffett Field, Calif.

REFERENCES

1. Smith, Willard G.: Wind-Tunnel Investigation of a 1/15-Scale Model of the Republic MX-1554 Airplane at Mach Numbers of 1.45 and 1.90. NACA RM SA53C17, 1953.

2. Lockwood, Vernard E., and Solomon, Martin: Stability and Control Characteristics at Low Speed of a 1/10-Scale Model of MX-1554A Design. NACA RM SL53A05, 1953.

TABLE I.- MODEL DIMENSIONS

Wing		
Area, sq in.		16.04
Span, in.		7.16
Mean aerodynamic chord, in.		2.99
Aspect ratio		3.20
Airfoil section		modified NACA 65A003
Sweepback of leading edge, deg		55
Sweepback of trailing edge, deg		10
Root chord, in.		4.48
Horizontal tail		
Area, sq in.		3.62
Span, in.		3.53
Aspect ratio		3.44
Sweepback of leading edge, deg		55
Sweepback of trailing edge, deg		15
Vertical tail	V_L	V_S
[1]Area, sq in.	6.41	5.22
[1]Span, in.	2.79	2.51
Sweepback of leading edge, deg	65	65
Sweepback of trailing edge, deg	26	26
Controls		
[2]Aileron area (one aileron only), sq in.		.63
[2]Elevator area, sq in.		1.22
[2]Rudder area, sq in.		1.11
Body		
Length, in.		14.41
Maximum width, in.		.86
Base area (excluding duct), sq in.		.54
Duct		
Inlet area, sq in.		.20
Exit area, sq in.		.29

[1]Measured from horizontal line through axis of duct exit
[2]Includes balance area

TABLE II.- AERODYNAMIC PARAMETERS OF A 1/60-SCALE MODEL OF THE REPUBLIC MX-1554 AIRPLANE AT $M_o = 2.85$

Configuration	$\frac{dC_L}{d\alpha}$ (per deg)	$(\alpha)_{C_L=0}$ (deg)	$\frac{dC_m}{dC_L}$	$(C_m)_{C_L=0}$	$C_{D_{min}}$	$\frac{dC_Y}{d\beta}$ (per deg)	$\frac{dC_n}{d\beta}$ (per deg)	$\frac{dC_l}{d\beta}$ (per deg)
B	0.0038	0.7	1.079	-0.002	0.0124	-0.0065	-0.0037	0.0001
BW	.0303	-.5	-.023	0	.0195	-.0065	-.0035	-.0002
BHV_S	.0073	.9	-.322	.001	.0156	-.0137	.0017	-.0009
$BWHV_S$	.0330	-.4	-.212	.003	.0218	-.0136	.0013	-.0008
$BWHV_L$	- - -	- - -	- - -	- - -	.0218	-.0156	.0025	-.0012

FIGURE LEGENDS

Figure 1.- System of axes.

Figure 2.- Three-view sketch of the 1/60-scale Republic MX-1554 airplane.

Figure 3.- Schlieren photographs of the body alone in pitch. (a) $\alpha = -5.1^{\circ}$. (b) $\alpha = -0.1^{\circ}$. (c) $\alpha = 4.9^{\circ}$.

Figure 4.- Aerodynamic characteristics in pitch of the Republic MX-1554 airplane. (a) Model buildup.

Figure 4.- Continued. (b) Effect of wing incidence on BW configuration.

Figure 4.- Continued. (c) Effect of wing incidence on $BWHV_S$ configuration.

Figure 4.- Continued. (d) Effect of horizontal-tail incidence on BHV_S configuration.

Figure 4.- Continued. (e) Effect of horizontal-tail incidence on $BWHV_S$ configuration.

Figure 4.- Continued. (f) Effect of elevator deflection on $BWHV_S$ configuration.

Figure 4.- Continued. (g) Effect of aileron deflection on $BWHV_S$ configuration.

Figure 4.- Concluded. (h) Effect of rudder deflection on BWHV configuration.

Figure 5.- Aerodynamic characteristics in sideslip of the Republic MX-1554 airplane. (a) Effect of adding the wing to the body.

Figure 5.- Continued. (b) Effect of adding the wing to the body and vertical tail.

Figure 5.- Continued. (c) Effect of adding the wing to the body and horizontal and vertical tail.

Figure 5.- Continued. (d) Effect of aileron deflection on $BWHV_S$ configuration.

Figure 5.- Continued. (e) Effect of rudder deflection on $BWHV_L$ configuration.

Figure 5.- Concluded. (f) Effect of vertical-tail size.

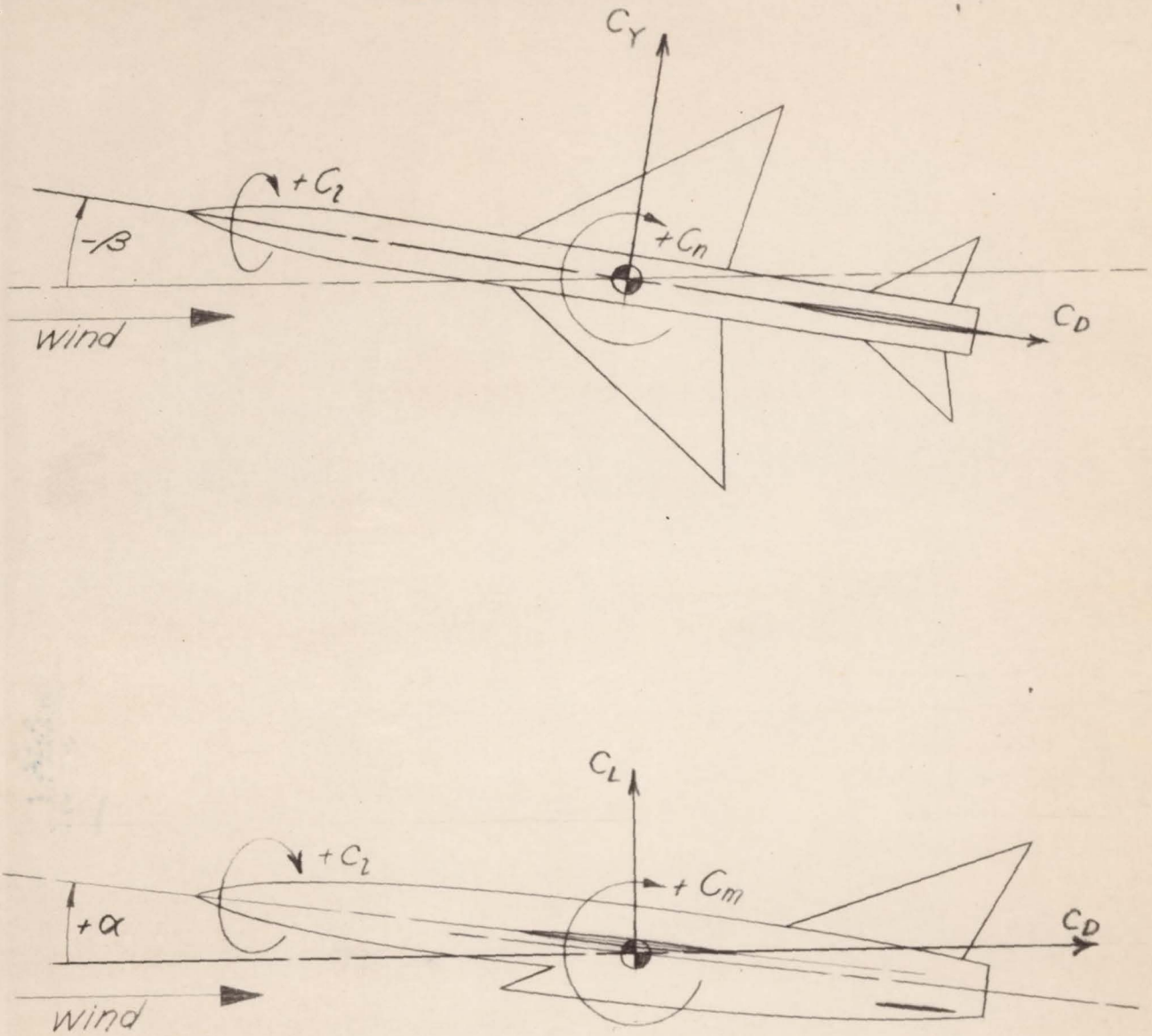

Figure 1.- System of axes.

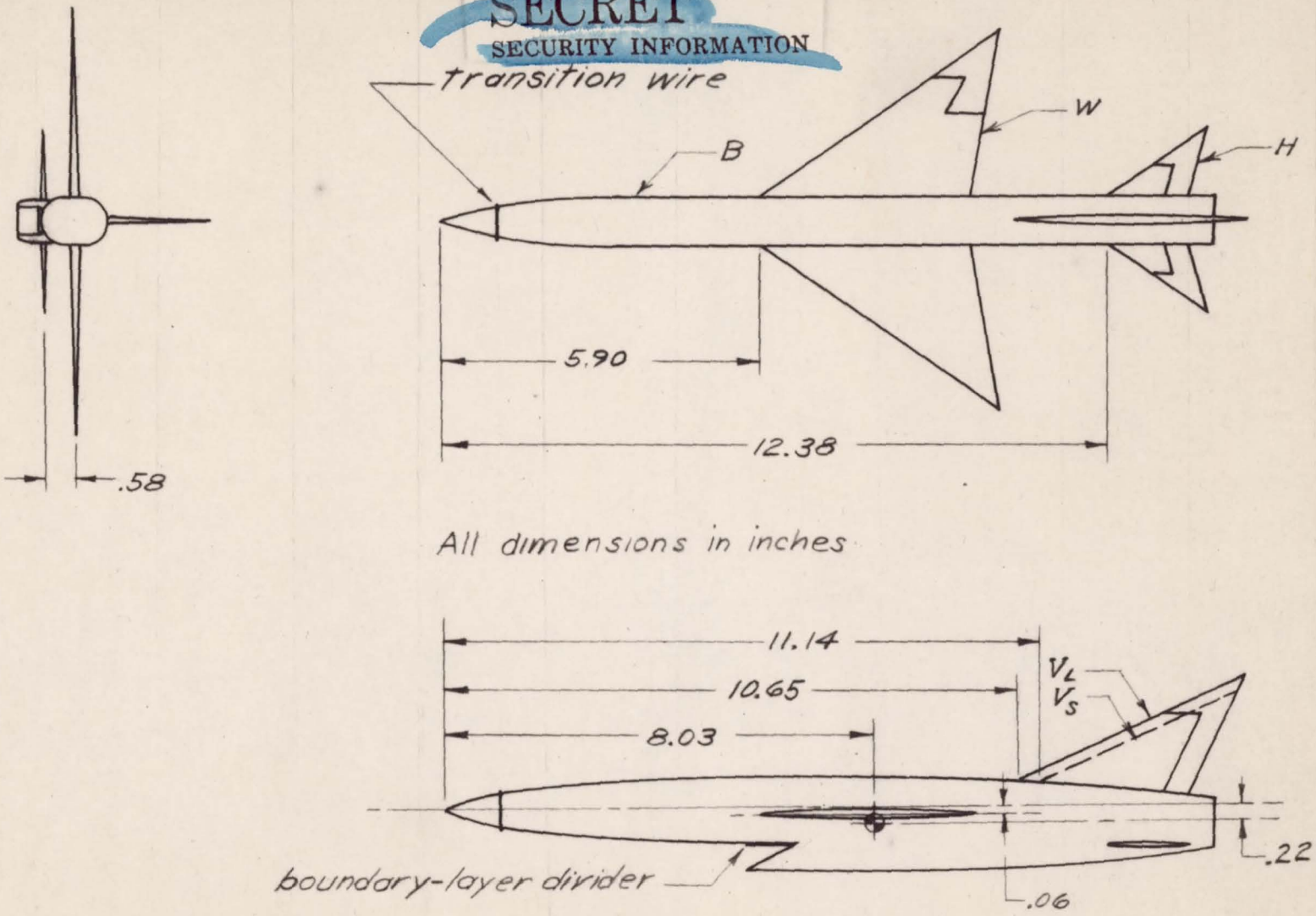

Figure 2.- Three-view sketch of the 1/60 - scale Republic MX-1554 airplane.

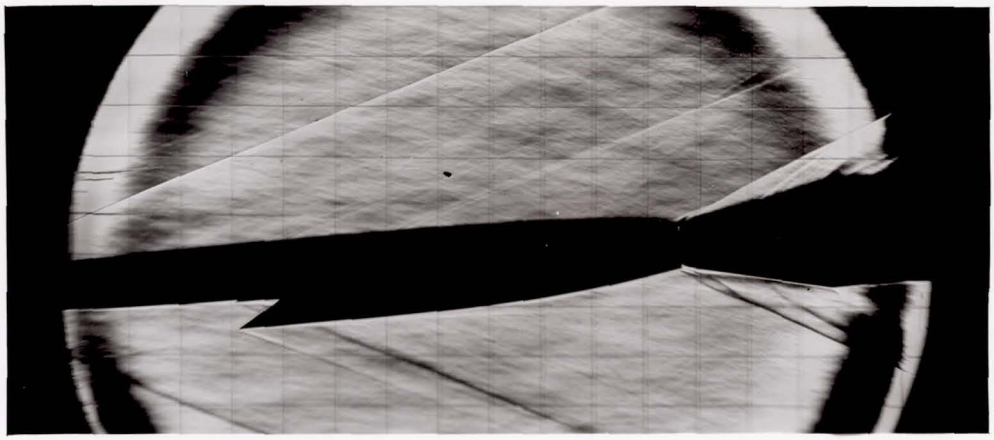

(a) $\alpha = -5.1^\circ$

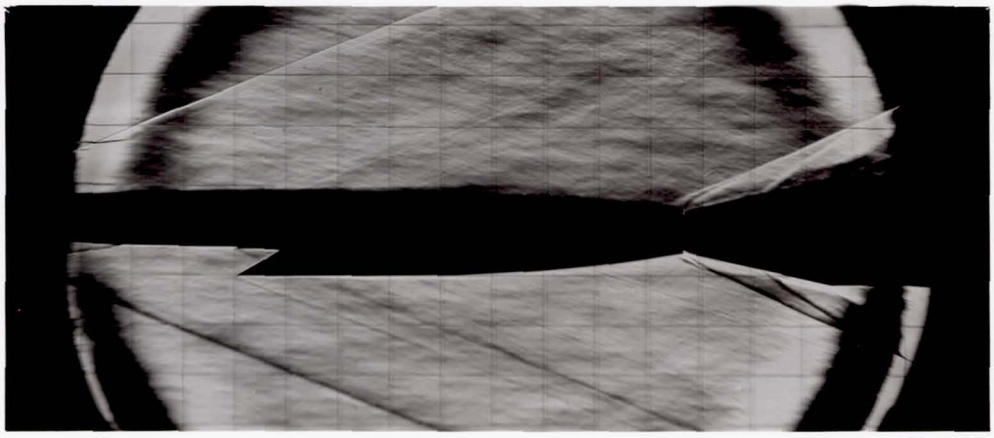

(b) $\alpha = -0.1^\circ$

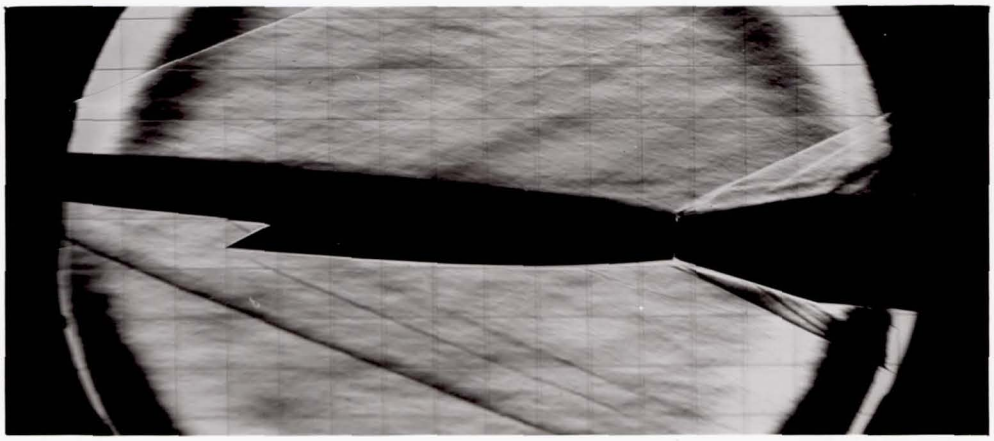

(c) $\alpha = 4.9^\circ$

NACA
A-17424

Figure 3.- Schlieren photographs of the body alone in pitch.

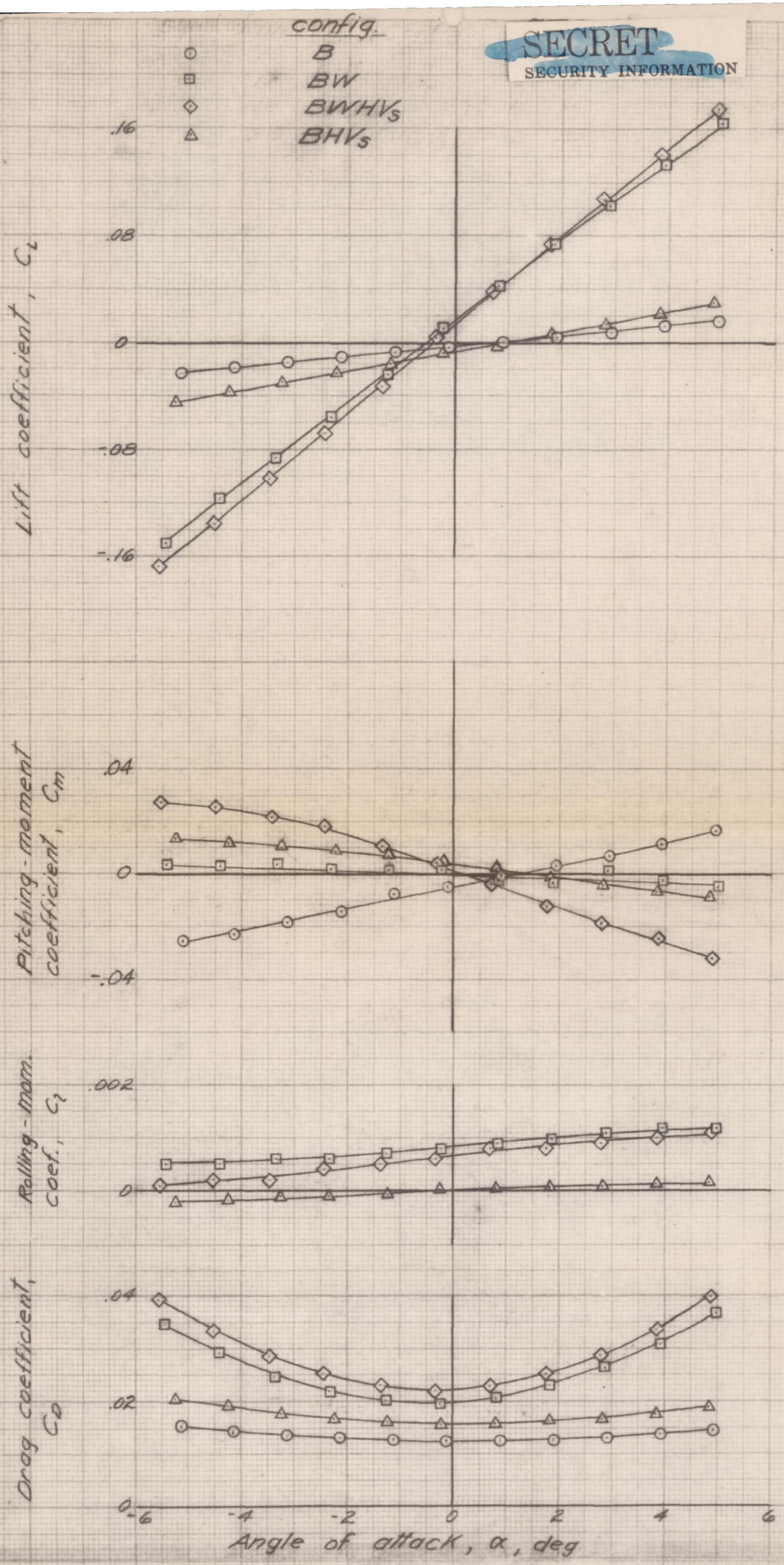

(a) Model buildup.

Figure 4.- Aerodynamic characteristics in pitch of the Republic MX-1554 airplane.

NACA RM SA50C11

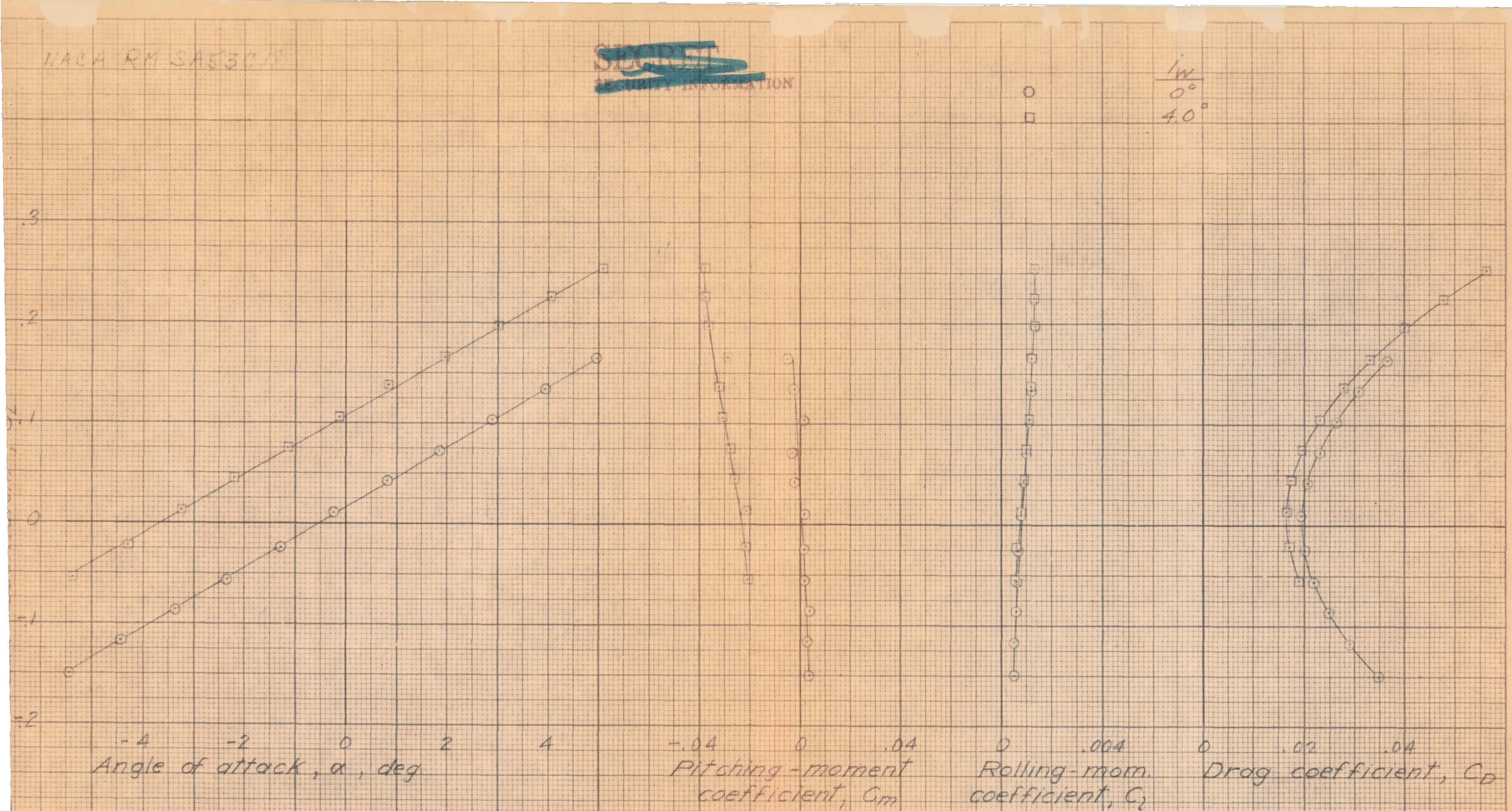

(b) Effect of wing incidence on BW configuration.

Figure 4. - Continued.

NACA RM L57E17

[redacted] CONFIDENTIAL

	i_w	i_H
○	0°	0°
□	4.0°	0°
◇	4.0°	4.0°

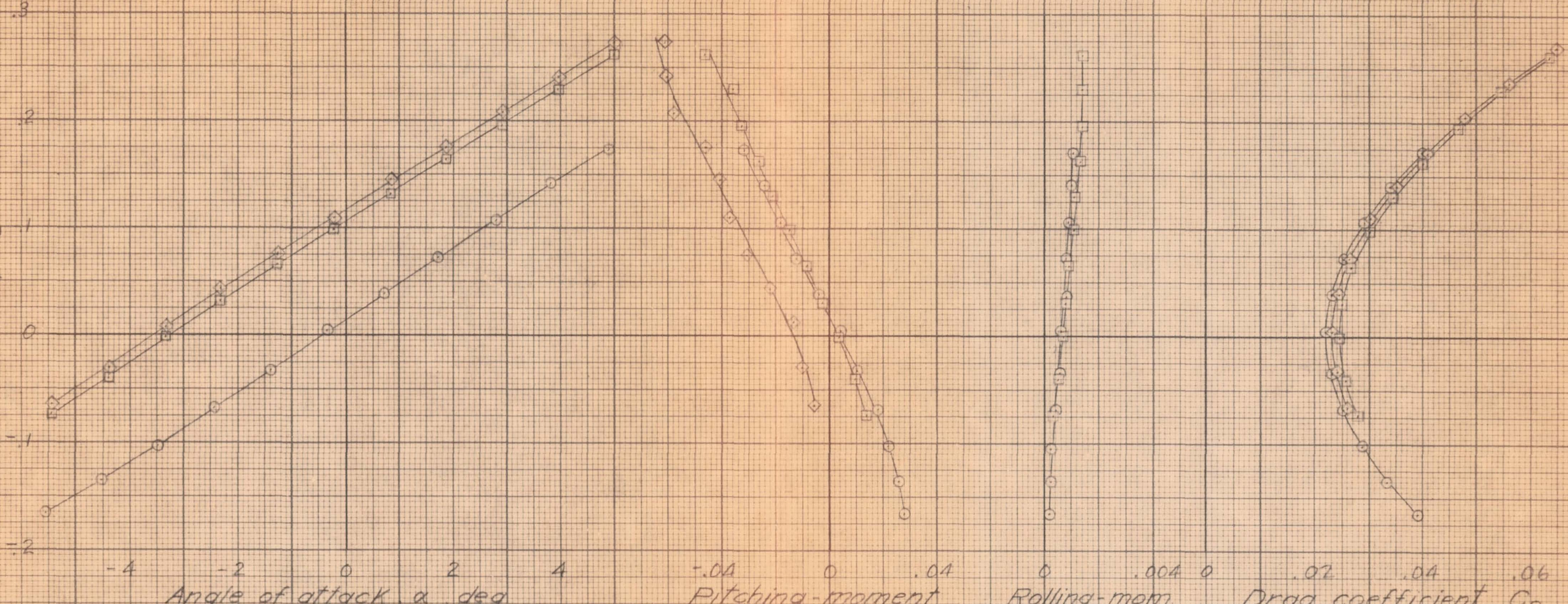

(c) Effect of wing incidence on BWHV$_S$ configuration.

Figure 4.- Continued.

[redacted] CONFIDENTIAL

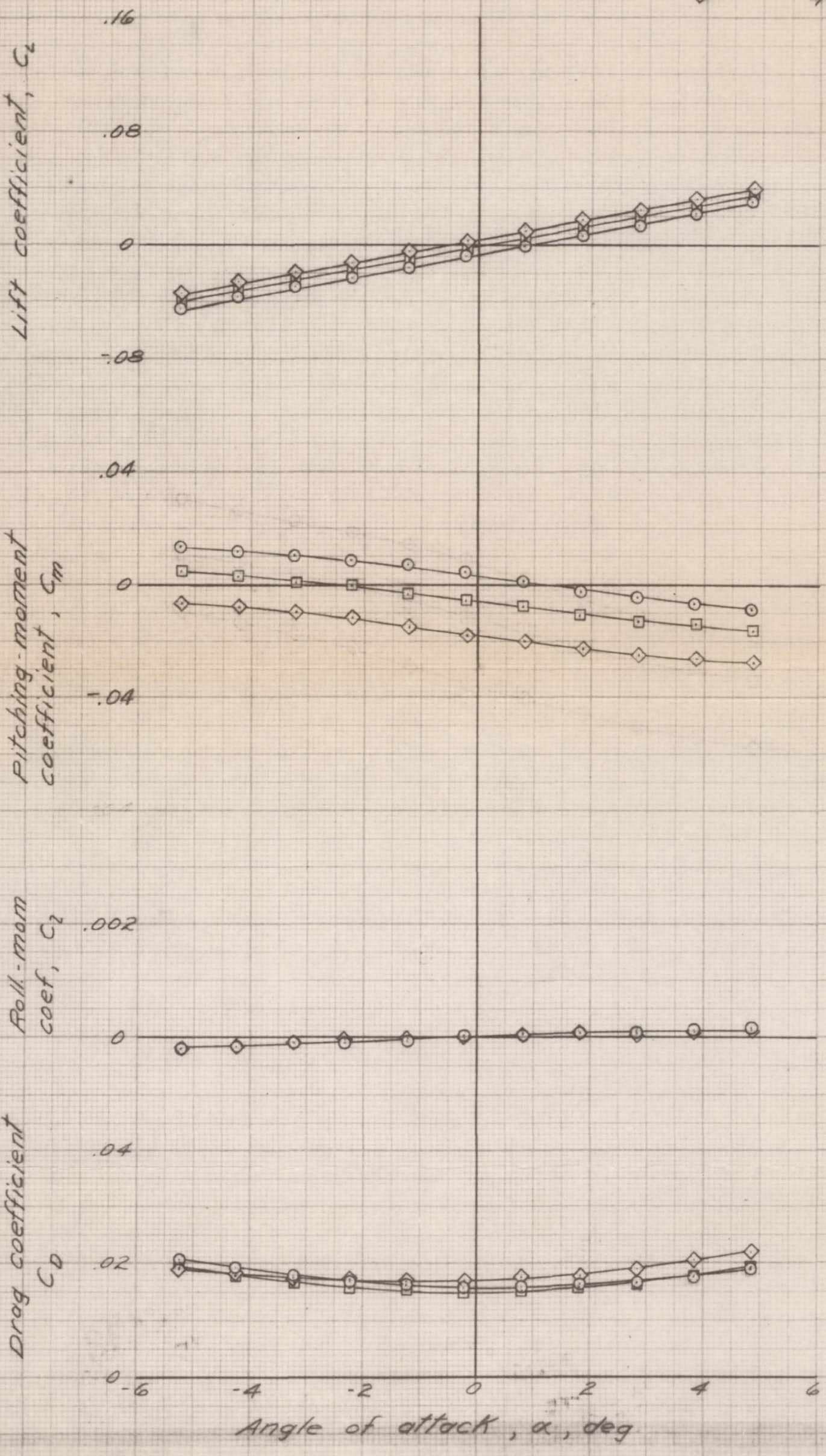

(d) Effect of horizontal-tail incidence on BHV$_5$ configuration.

Figure 4.- Continued.

NACA-LMA SAFSCIB

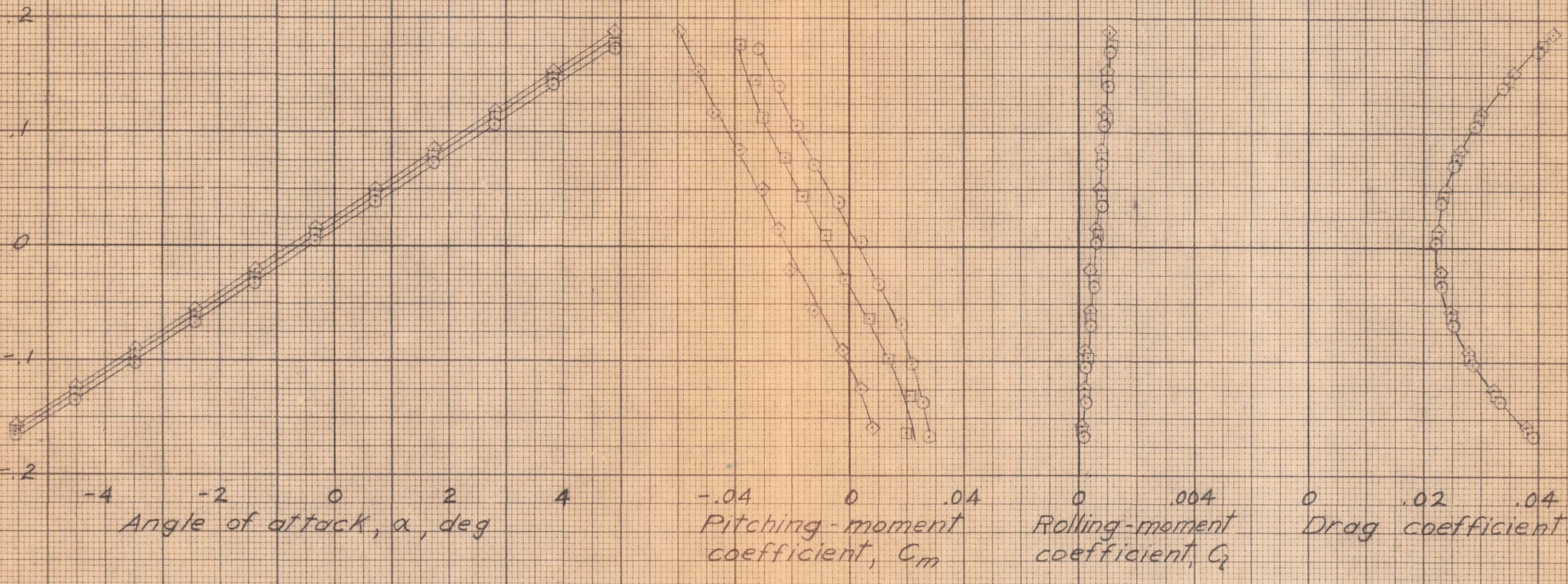

(e) Effect of horizontal tail incidence on B(W)HV_S configuration.

Figure 4 - Continued.

NASA RM SA52E15

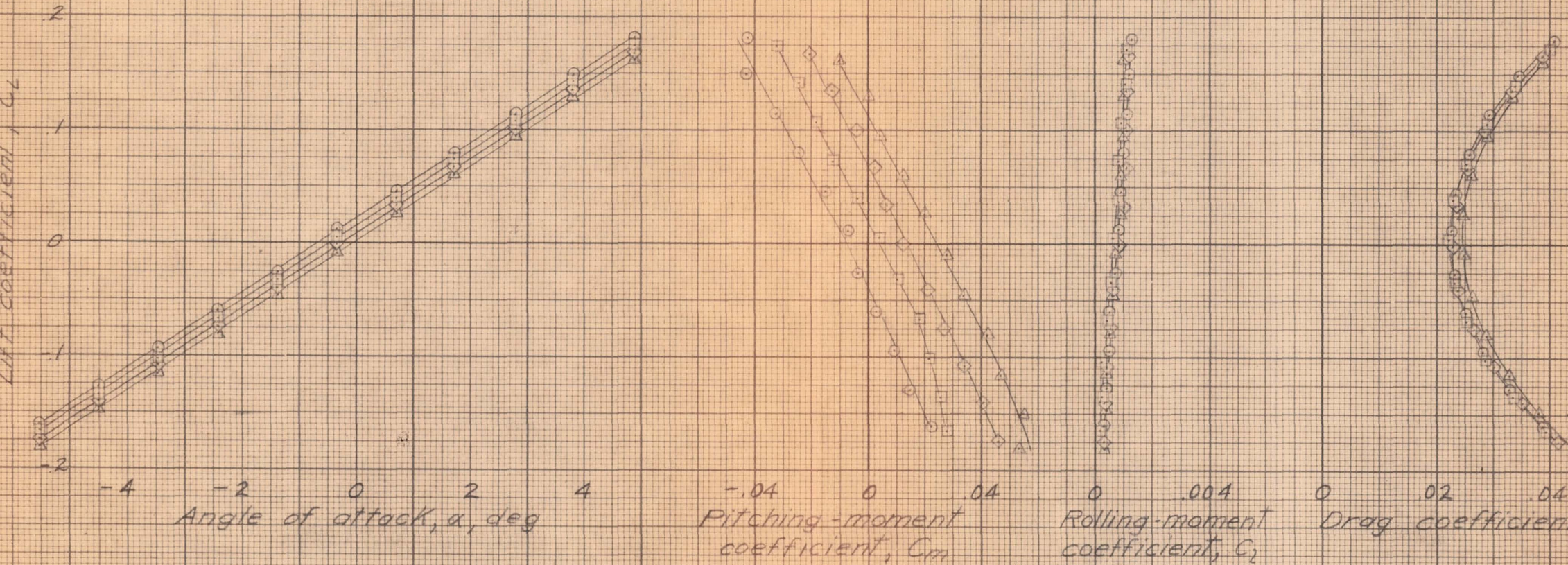

(f) Effect of elevator deflection on BWHV$_S$ configuration.

Figure 4.- Continued.

NACA RM S55E18

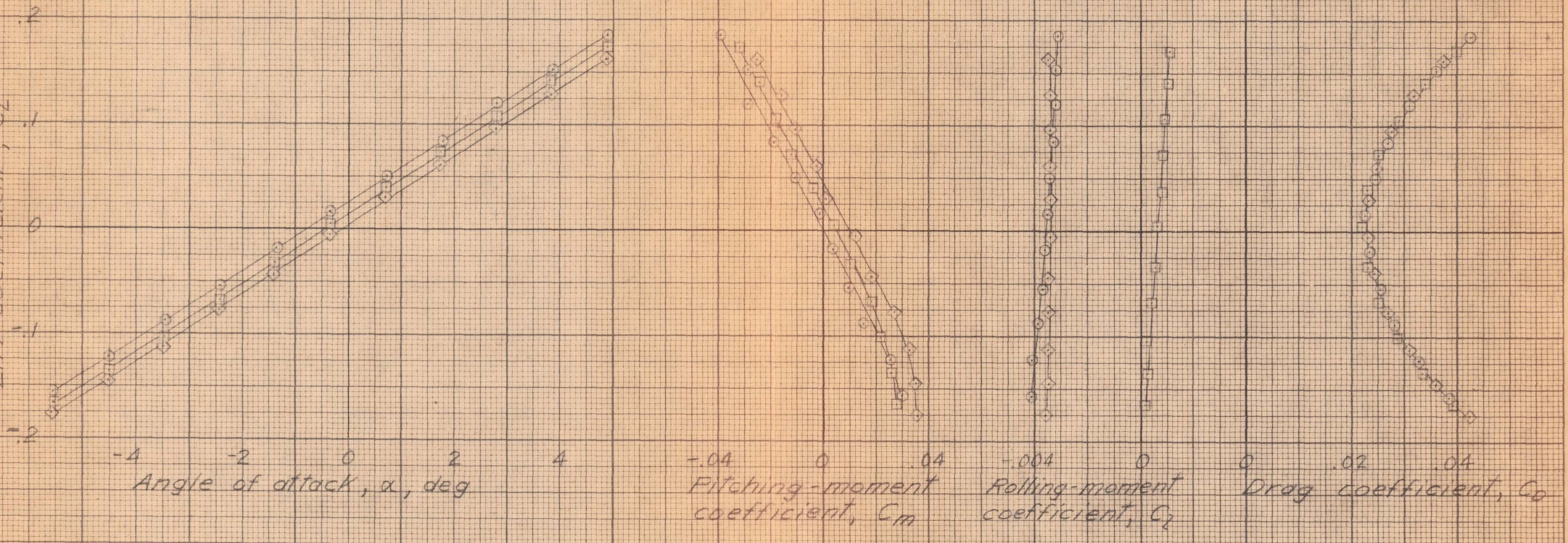

(g) Effect of aileron deflection on BWHV$_S$ configuration.

Figure 4.- Continued

NACA RM SA53C18

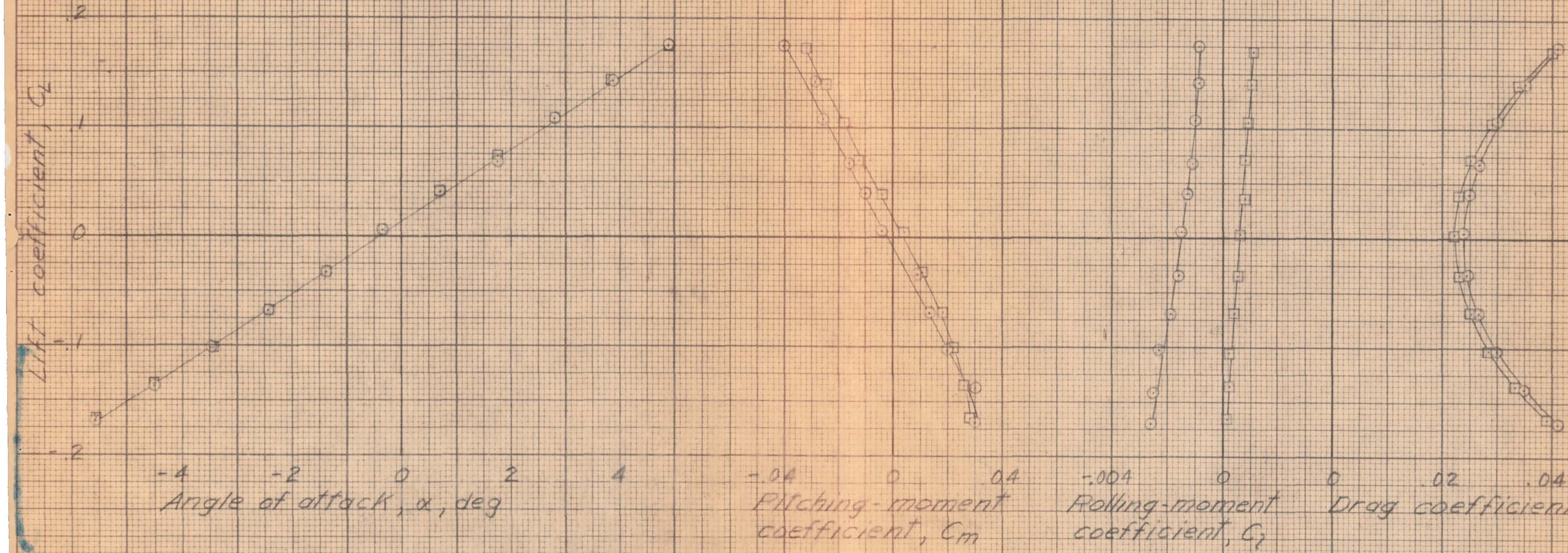

(h) Effect of rudder deflection on BWHV configuration.

Figure 4.- Concluded.

Config.
B
BW

NACA RM SA53C18

Side-force coefficient, C_Y

.08
.04
0
-.04

Yawing-moment coefficient, C_n

.01
0
-.01

Rolling-moment coefficient, C_l

.004
0
-.004

Drag coefficient, C_D

.02
0

-6 -4 -2 0 2 4 6

Sideslip angle, β, deg

(a) Effect of adding the wing to the body.

Figure 5.- Aerodynamic characteristics in sideslip of the Republic XF-15S4 airplane.

A5-8a

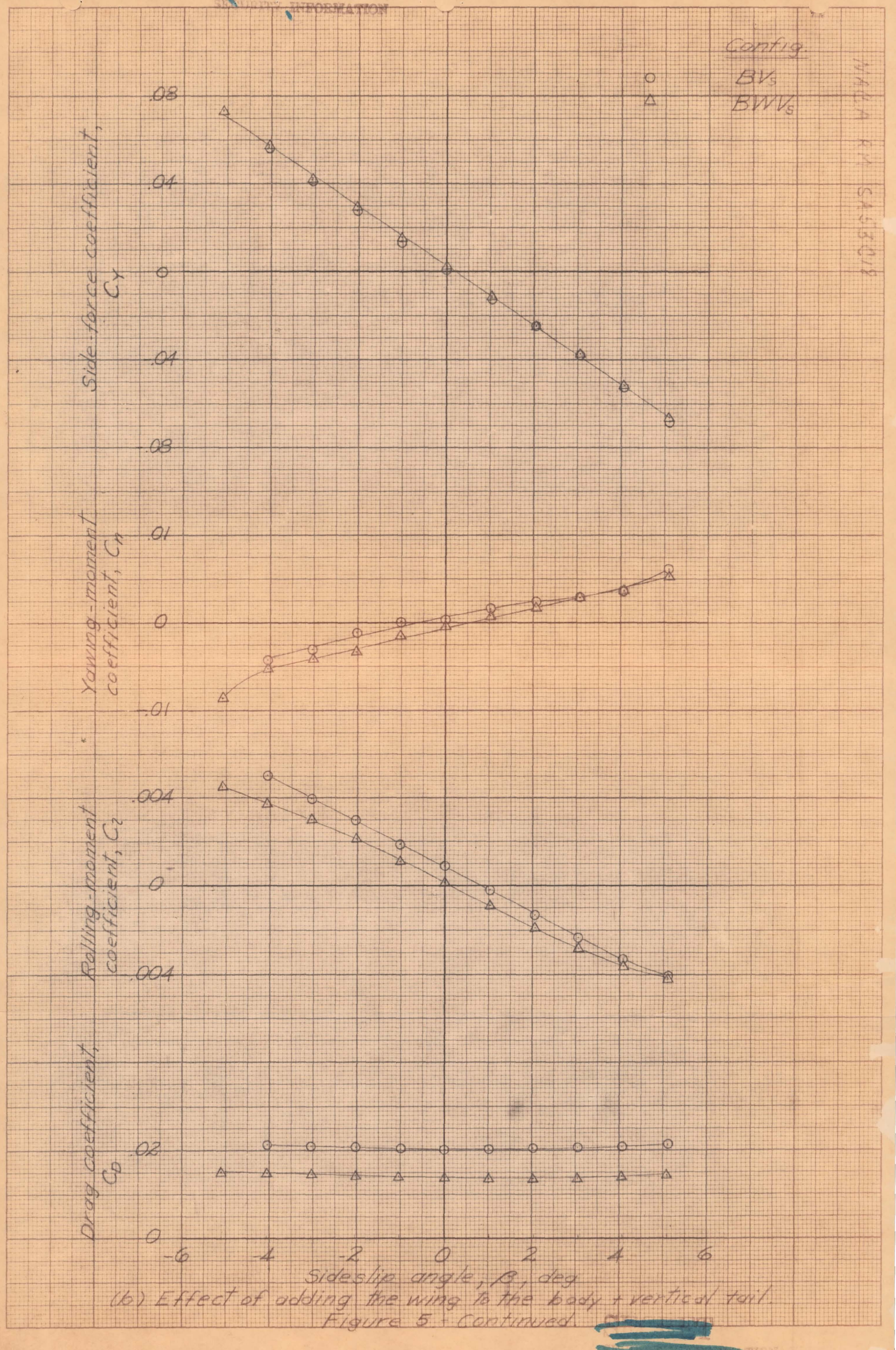

(b) Effect of adding the wing to the body + vertical tail.

Figure 5.- Continued.

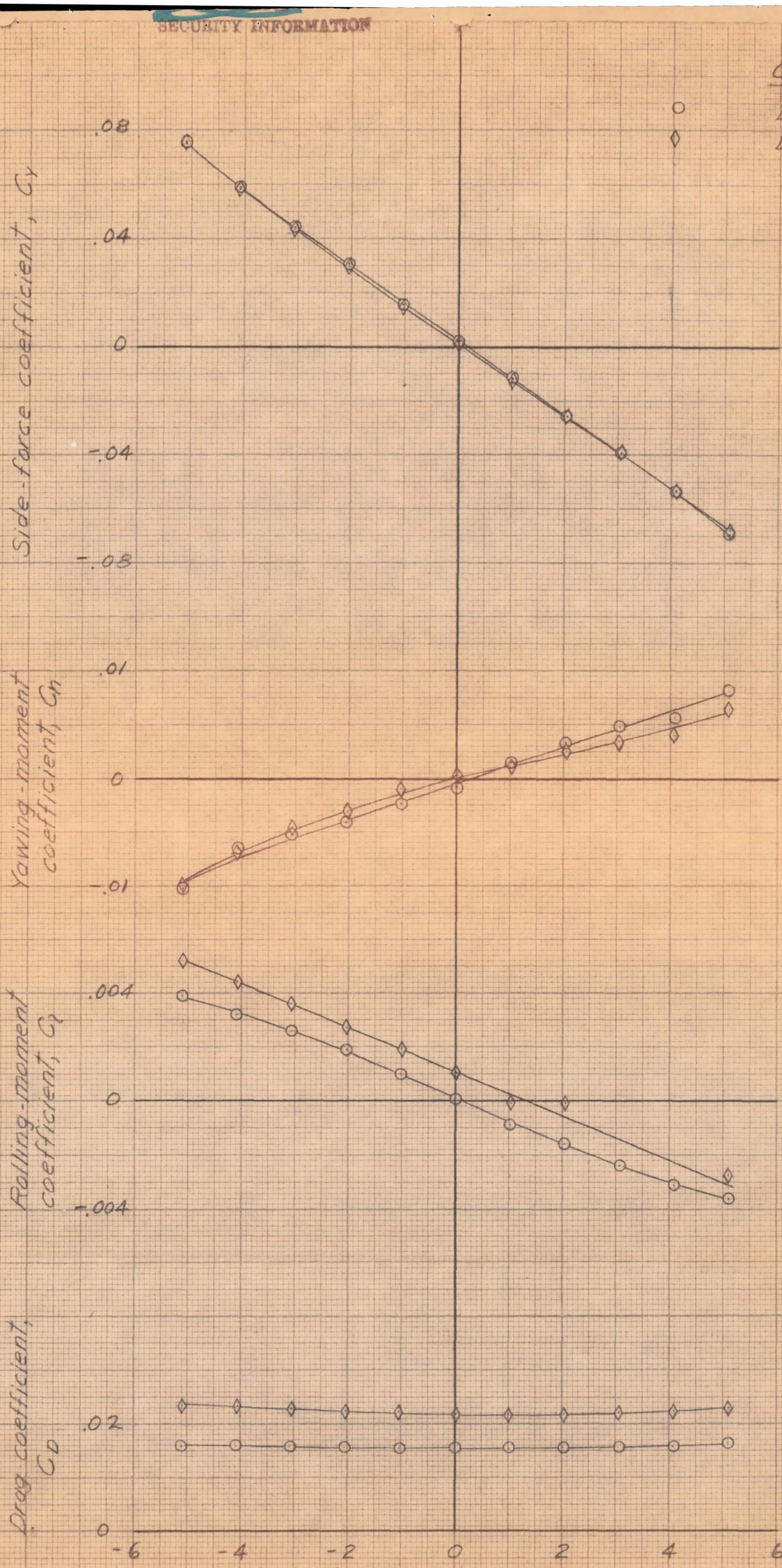

(c) Effect of adding the wing to the body + horiz. and vertical tail.

Figure 5.- Continued.

	Right aileron δ_a	Left aileron δ_a
○	0°	0°
□	4.2°	0°
◇	0°	-4.2°
△	0°	-10.4°

Side-force coefficient, C_Y

.08
.04
0
-.04
-.08

Yawing-moment coefficient, C_n

-.01
0
.01

Rolling-moment coefficient, C_l

.004
0
-.004

Drag coefficient, C_D

.02
0

-6 -4 -2 0 2 4 6

Sideslip angle, β, deg

(d) Effect of aileron deflection on BWHV$_s$ configuration.

Figure 5. - Continued.

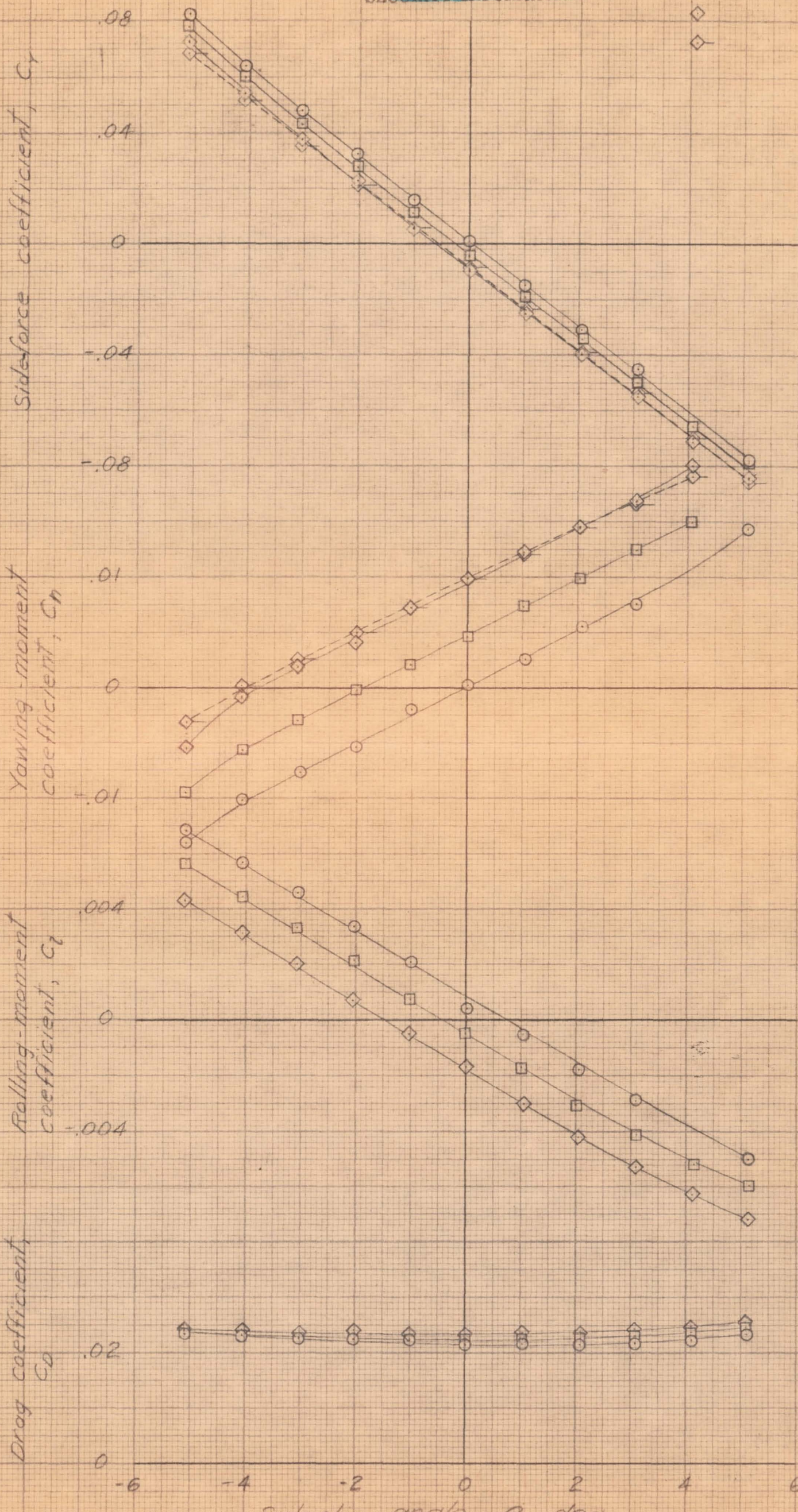

(e) Effect of rudder deflection on BWHV$_L$ configuration.

Figure 5.- Continued.

Config.
BWHV$_S$
BWHV$_L$

Side-force coefficient, C_Y
.08
.04
0
-.04
-.08

Yawing-moment coefficient, C_n
.01
0
-.01

Rolling-moment coefficient, C_l
.004
0
-.004

Drag coefficient, C_D
.02
0

-6 -4 -2 0 2 4 6
Sideslip angle, β, deg

(f) Effect of vertical-tail size.

Figure 5.- Concluded.